JS 25

METROLOGY AT THE HEART OF TODAY'S TECHNOLOGIES

Mushroom multi-vias pour des structures empilées à bande interdite avec symétrie de réflexion glissé

Stacked Multi-Via Mushroom-Type EBG Structures with Glide Symmetry

Ashray Ugle[1,2], Massimiliano Casaletti[1,2], Marta Arias Campo[3], Simona Bruni[3], Guido Valerio[1,2]

[1] *Sorbonne Université, Laboratorie de Génie Électrique et Électronique de Paris (GeePs), 75005, Paris, France,* ashray.ugle@sorbonne-universite.fr, massimiliano.casaletti@sorbonne-universite.fr, guido.valerio@sorbonne-universite.fr

[2] *Université Paris-Saclay, CentraleSupélec, CNRS, GeePs, 91192, Gif-sur-Yvette, France*

[3] *Department of Antennas & EM Modelling, IMST GmbH, 47475, Kamp-Lintfort, Germany,* simona.bruni@imst.de, marta.arias@imst.de

Mots-clés / Keywords: Analyse de dispersion / Dispersion analysis, Matériaux à bande interdite électromagnétique / Electromagnetic bandgap materials, Symétrie de réflexion glissé / Glide symmetry, Analyse multimodale / Multimodal analysis.

Résumé/Abstract

Cette étude examine la dispersion de structures à bande interdite électromagnétique (EBG) de type mushroom empilées avec multi-vias, intégrant une symétrie de glissement, dans la plage de fréquences de 50 à 90 GHz. Il est observé que la cellule élémentaire innovante à symétrie de réflexion glissée peut fonctionner comme une structure EBG indépendamment du nombre de couches empilées. En utilisant la méthode matricielle de transfert multi-modale (MMTMM), le nombre d'onde complexe de la structure périodique est obtenu par post-traitement des paramètres *S* généralisés issus d'un solveur commercial. Les résultats mettent en évidence que les structures EBG de type mushroom empilées avec multi-vias et symétrie de réflexion glissée offrent des avantages significatifs pour la conception de composants de guides d'ondes à fente, en utilisant une technologie de circuits imprimés (PCB) multicouches économique.

The presented study investigates the dispersion behaviour of stacked multi-via mushroom-type electromagnetic bandgap (EBG) structures with glide symmetry in the 50-90 GHz frequency range. It is observed that the novel glide-symmetric unit cell is able to function as an EBG independent of the number of layers when stacked. Using the multi-mode transfer matrix method (MMTMM), the complex wavenumber of the unit cells is obtained by post-processing the generalised S-Parameters from a commercial solver. The findings highlight that the stacked multi-via mushroom-type EBG structures with glide symmetry offer significant advantages in the design of gap-waveguide components using cost-effective multi-layer printed circuit board (PCB) technology.

1 Introduction

The growing advancement in millimeter-wave (mm-Wave) automotive radar technology [1], [2] has increased the demand for low-loss and cost-effective antenna and waveguide solutions. While traditional metallic waveguide technology offers minimal losses, they are expensive to manufacture. PCB based solutions are cost-efficient but suffer from high material losses in this frequency range. Gap waveguide technology [3], realised with PCB based EBG structures combines the advantages of both technologies. Mushroom-type EBGs [4] have been proven to be effective in PCB configurations [5]-[8], but suffer a reduction in stopband bandwidth when stacked [9], [10], as the number of layers increase. Also, the studies in [4]-[10] have been conducted primarily at lower frequencies. A periodic structure is said to be glide-symmetric, if it is invariant after a translation by half the period followed by a reflection. Recently, periodic structures with glide symmetry have been shown to produce wide stopbands [11] and they were used in [12] to improve the stopband bandwidth of mushroom-type EBGs. To address the challenges of stacking in the 50-90 GHz range, a glide-symmetric EBG cell has been investigated to maintain its stopband performance in stacked configurations, making it ideal for multi-layer PCB based gap-waveguides.

2 Modelling Methodology

The conventional mushroom-type EBG is modified with multiple vias, and glide-symmetry is introduced to be enclosed in a parallel plate waveguide (PPW) environment as shown in Figure 1a. The dispersion characteristics of the proposed multi-via glide-symmetric mushroom-type EBG are analysed using MMTMM [13], [14]. To compute the complex wavenumber of a 2-D periodic structure using MMTMM, the unit cell is simulated in CST using frequency domain solver [16] with N waveguide modes on each of the four faces, to account for the interactions from the adjacent cells. The multi-mode transfer matrix $[\mathbf{T}]$ of size $4N \times 4N$ can be obtained from the generalised scattering parameters from CST, and can be used to solve a non-standard eigenvalue problem in the form of

$$[\mathbf{T}]\begin{bmatrix}\mathbf{V}_x\\ \mathbf{V}_y\\ \mathbf{I}_x\\ \mathbf{I}_y\end{bmatrix} = \begin{bmatrix}\lambda_x\mathbf{V}_x\\ \lambda_y\mathbf{V}_y\\ \lambda_x\mathbf{I}_x\\ \lambda_y\mathbf{I}_y\end{bmatrix};\ [\mathbf{T}] = \begin{bmatrix}[\mathbf{A}] & [\mathbf{B}]\\ [\mathbf{C}] & [\mathbf{D}]\end{bmatrix}, \tag{1}$$

where $\lambda_i = \mathrm{e}^{-\mathrm{j}k_i p_i}; i = x, y$, such that, k_i is the complex wavenumber and p_i is the periodicity along the i direction. The multi-mode transfer matrix $[\mathbf{T}]$ consists of four submatrices $[\mathbf{A}], [\mathbf{B}], [\mathbf{C}], [\mathbf{D}]$ of sizes $N \times N$, respectively. The complex wavenumber $k_i = \beta_i - \mathrm{j}\alpha_i; i = x.y$ contains the phase constant β_i and attenuation constant α_i along the i direction. The eigenvalue problem in (1) is non-standard, and can be solved using root-finding algorithms or by following a linearisation procedure as in [15], the latter of which is employed in this work. After employing the linearisation procedure, the eigenvalue problem in (1) can be modified as

$$[\widetilde{\mathbf{T}}]\begin{bmatrix}\mathbf{V}_x\\ \mathbf{I}_x\\ \mathbf{V}_y\\ \mathbf{I}_y\end{bmatrix} = \begin{bmatrix}\lambda_x\mathbf{V}_x\\ \lambda_x\mathbf{I}_x\\ \lambda_y\mathbf{V}_y\\ \lambda_y\mathbf{I}_y\end{bmatrix};\ [\widetilde{\mathbf{T}}] = \begin{bmatrix}[\widetilde{\mathbf{T}}_{xx}] & [\widetilde{\mathbf{T}}_{xy}]\\ [\widetilde{\mathbf{T}}_{yx}] & [\widetilde{\mathbf{T}}_{yy}]\end{bmatrix}, \tag{2}$$

where $[\mathbf{T}]$ is permuted as $[\widetilde{\mathbf{T}}] = [\mathbf{P}][\mathbf{T}][\mathbf{P}]$ with a suitable permutation matrix $[\mathbf{P}]$. This procedure results in two standard eigenvalue problems

$$\{[\widetilde{\mathbf{T}}_{xx}] + [\widetilde{\mathbf{T}}_{xy}][\mathbf{Q}_x][\widetilde{\mathbf{T}}_{yx}]\}\begin{bmatrix}\mathbf{V}_x\\ \mathbf{I}_x\end{bmatrix} = \lambda_x\begin{bmatrix}\mathbf{V}_x\\ \mathbf{I}_x\end{bmatrix}, \tag{3}$$

$$\{[\widetilde{\mathbf{T}}_{yy}] + [\widetilde{\mathbf{T}}_{yx}][\mathbf{Q}_y][\widetilde{\mathbf{T}}_{xy}]\}\begin{bmatrix}\mathbf{V}_y\\ \mathbf{I}_y\end{bmatrix} = \lambda_y\begin{bmatrix}\mathbf{V}_y\\ \mathbf{I}_y\end{bmatrix}, \tag{4}$$

such that

$$[\mathbf{Q}_x] = \left(\lambda_y[\mathbf{1}] - [\widetilde{\mathbf{T}}_{xx}]\right)^{-1} \tag{5}$$

$$[\mathbf{Q}_y] = \left(\lambda_x[\mathbf{1}] - [\widetilde{\mathbf{T}}_{yy}]\right)^{-1} \tag{6}$$

where $[\mathbf{1}]$ is an identity matrix of size $N \times N$.

The complex wavenumber for the glide-symmetric mushroom-type EBG structure is then computed in the irreducible Brillouin zone. By fixing λ_y and λ_x in (5) and (6), respectively, The eigenvalue problems in (3) and (4) can be solved to obtain k_x for the $\overline{\Gamma\mathrm{X}}$ segment and k_y for the $\overline{\mathrm{XM}}$ segment. For the $\overline{\mathrm{M}\Gamma}$ segment, the eigenvalue problem in (1) is already linear, and can be solved directly since $k_x = k_y$.

3 Results and Discussion

The dispersion diagram for the unit cell in Figure 1a in the irreducible Brillouin zone computed using MMTMM with $N = 5$ modes for the glide-symmetric multi-via mushroom-type EBG in Figure 1a is compared with CST eigenmode solver (ES) in Figure 1b. The MMTMM computation shows good agreement with the CST ES results with a stopband observed from 43 to 93 GHz. The normalised attenuation constants obtained using MMTMM in the $\overline{\Gamma\mathrm{X}}$ and $\overline{\mathrm{M}\Gamma}$ directions, is shown in Figure 1c. The minimum of the two constants is highlighted in red, depicting the minimum attenuation in the stopband.

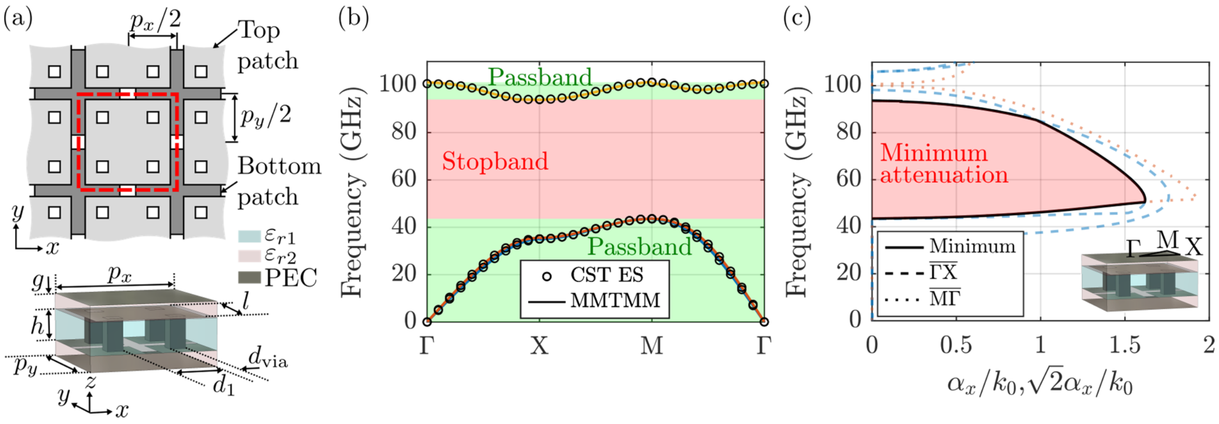

Figure 1: (a) Multi-via mushroom-type EBG with glide symmetry inside a PPW environment with dimensions $p_x = 0.8$ mm, $p_y = 0.8$ mm, $g = 0.04$ mm, $h = 0.2$ mm, $l = 0.7$ mm, $d_{via} = 0.1$ mm, $d_1 = 0.3$ mm and material properties $\varepsilon_{r1}, \varepsilon_{r2} = 4.4$. (b) Normalised phased constant in the irreducible Brillouin zone, with the stopband and passband regions shaded in red and green, respectively. (c) Normalised attenuation constants in the $\overline{\Gamma X}$ and $\overline{M\Gamma}$ direction, showing the minimum of the two constants in red.

The easiest way to stack the EBG structure in Figure 1a is to simply translate the unit cell vertically. No stopband is observed when stacked by translation. However, when the unit cell in Figure 1a is stacked by performing a mirror operation, as shown in Figure 2a, the stopband is retained. The dispersion diagram in the irreducible Brillouin zone for the stacked structure in Figure 2b is computed using MMTMM ($N = 5$) and is compared with CST ES in Figure 2b. Once again, the MMTMM calculation coincides well with the CST ES results. The normalised attenuation constants calculated with MMTMM in the $\overline{\Gamma X}$ and $\overline{M\Gamma}$ directions with the minimum of the two, highlighted in red, is shown in Figure 2c. It is observed that both the stopband width and minimum attenuation of the stacked structure is preserved, making it well-suited for multi-stacked gap waveguide components realised using PCB technology.

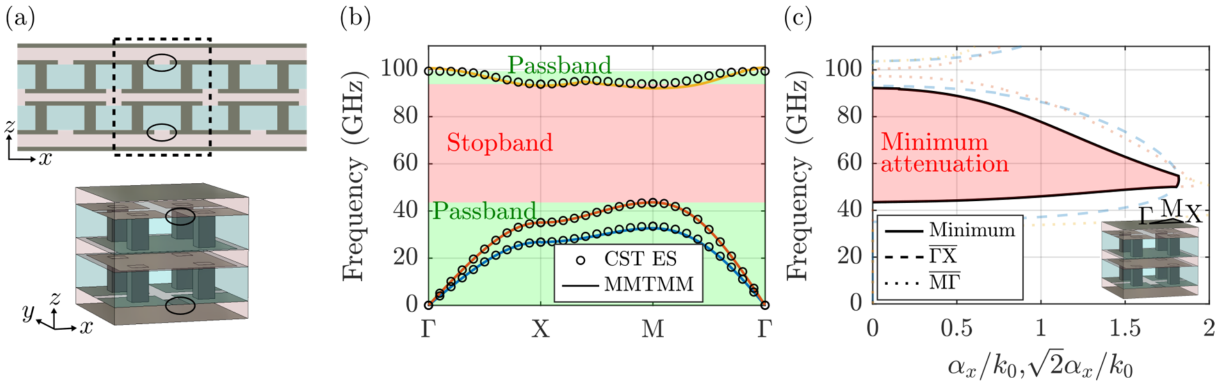

Figure 2: (a) Stacking of the EBG structure inside a PPW environment in Figure 1a using mirroring. (b) Normalised phased constant in the irreducible Brillouin zone, with the stopband and passband regions shaded in red and green, respectively. (c) Normalised attenuation constants in the $\overline{\Gamma X}$ and $\overline{M\Gamma}$ direction, showing the minimum of the two constants in red.

4 Conclusion

This study presents a novel stacked multi-via mushroom-type EBG with glide symmetry whose stopband is unaffected when stacked in a mirrored configuration. The results demonstrate its suitability for multi-layer PCB-based gap waveguide components for low-loss and low-cost implementations in mm-Wave automotive radar.

Acknowledgement

This publication is based upon work supported by the Horizon Europe Research and Innovation Program and UKRI under the GENIUS Project, Marie Skłodowska-Curie Grant under Agreement 101072560.

References

[1] C. Waldschmidt, J. Hasch, and W. Menzel, “Automotive radar — from first efforts to future systems,” IEEE Journal of Microwaves, vol. 1, no. 1, pp. 135–148, 2021.

[2] J. Hasch, E. Topak, R. Schnabel, T. Zwick, R. Weigel, and C. Waldschmidt, “Millimeter-wave technology for automotive radar sensors in the 77 ghz frequency band,” IEEE Transactions on Microwave Theory and Techniques, vol. 60, no. 3, pp. 845–860, 2012.

[3] E. Rajo-Iglesias, M. Ferrando-Rocher, and A. U. Zaman, “Gap waveguide technology for millimeter-wave antenna systems,” IEEE Communications Magazine, vol. 56, no. 7, pp. 14–20, 2018.

[4] D. Sievenpiper, L. Zhang, R. Broas, N. Alexopolous, and E. Yablonovitch, “High-impedance electromagnetic surfaces with a forbidden frequency band,” IEEE Transactions on Microwave Theory and Techniques, vol. 47, no. 11, pp. 2059–2074, 1999.

[5] S. Rogers, “Electromagnetic-bandgap layers for broad-band suppression of tem modes in power planes,” IEEE Transactions on Microwave Theory and Techniques, vol. 53, no. 8, pp. 2495–2505, 2005.

[6] E. Pucci, E. Rajo-Iglesias, and P.-S. Kildal, “New microstrip gap waveguide on mushroom-type ebg for packaging of microwave components,” IEEE Microwave and Wireless Components Letters, vol. 22, no. 3, pp. 129–131, 2012.

[7] C.-D. Wang, Y.-M. Yu, F. de Paulis, A. C. Scogna, A. Orlandi, Y.-P. Chiou, and T.-L. Wu, “Bandwidth enhancement based on optimized via location for multiple vias ebg power/ground planes,” IEEE Transactions on Components, Packaging and Manufacturing Technology, vol. 2, no. 2, pp. 332–341, 2012.

[8] N. Bayat-Makou and A. A. Kishk, “Contactless air-filled substrate integrated waveguide,” IEEE Transactions on Microwave Theory and Techniques, vol. 66, no. 6, pp. 2928–2935, 2018.

[9] M. A. M. Hassan and A. A. Kishk, “Bandwidth study of the stacked mushroom ebg unit cells,” IEEE Transactions on Antennas and Propagation, vol. 65, no. 8, pp. 4357–4362, 2017.

[10] X.-F. Zhao, J.-Y. Deng, J.-Y. Yin, D. Sun, L.-X. Guo, X.-H. Ma, and Y. Hao, “Novel suspended-line gap waveguide packaged with stacked-mushroom ebg structures,” IEEE Transactions on Microwave Theory and Techniques, vol. 69, no. 5, pp. 2447–2457, 2021.

[11] O. Quevedo-Teruel, Q. Chen, F. Mesa, N. J. G. Fonseca, and G. Valerio, “On the benefits of glide symmetries for microwave devices,” IEEE Journal of Microwaves, vol. 1, no. 1, pp. 457–469, 2021.

[12] B. A. Mouris, A. Fernández-Prieto, R. Thobaben, J. Martel, F. Mesa, and O. Quevedo-Teruel, “On the increment of the bandwidth of mushroom-type ebg structures with glide symmetry,” IEEE Transactions on Microwave Theory and Techniques, vol. 68, no. 4, pp. 1365–1375, 2020.

[13] F. Mesa, G. Valerio, R. Rodríguez-Berral, and O. Quevedo-Teruel, “Simulation-assisted efficient computation of the dispersion diagram of periodic structures: A comprehensive overview with applications to filters, leaky-wave antennas and metasurfaces,” IEEE Antennas and Propagation Magazine, vol. 63, no. 5, pp. 33–45, 2021.

[14] M. Bagheriasl, O. Quevedo-Teruel, and G. Valerio, “Bloch analysis of artificial lines and surfaces exhibiting glide symmetry,” IEEE Transactions on Microwave Theory and Techniques, vol. 67, no. 7, pp. 2618–2628, 2019.

[15] F. Giusti, Q. Chen, F. Mesa, M. Albani, and O. Quevedo-Teruel, “Efficient bloch analysis of general periodic structures with a linearized multimodal transfer-matrix approach,” IEEE Transactions on Antennas and Propagation, vol. 70, no. 7, pp. 5555–5562, 2022.

[16] “CST Studio Suite 3D Electromagnetic Analysis Software Package.” https://www.3ds.com/products/simulia/cst-studio-suite.